

CLUSTER MASS PROFILE FROM LENSING

Hanadi AbdelSalam, Prasenjit Saha

Astrophysics, Department of Physics, Keble Rd., OX1 3RH, Oxford, UK

Liliya L.R. Williams

Institute of Astronomy, Madingley Rd., CB3 0HA, Cambridge, UK

We propose a new technique to reconstruct non-parametrically the projected mass distribution of galaxy clusters from their gravitational lens effect on background galaxies. The beauty of our technique, is that it combines information from multiple imaging (strong lensing) and shear (weak lensing) as linear constraints on the projected mass distribution. Moreover, our technique overcomes all the drawbacks of non-linear methods. The method is applied to the first cluster-lens A370 and to the cluster-lens A2218 which is exceptionally rich in multiple images and arc(let)s. The reconstructed maps for both cases revealed unprecedented level of details.

1 Introduction

Gravitational lensing provides us with the necessary information (constraints) needed for probing the matter distribution of cosmic lenses. We present a new technique that combines information from strong and weak lensing in a linear fashion and reconstructs mass maps that follows the cluster light distribution as closely as possible while strictly preserving the lensing constraints. Our technique overcomes many of the drawbacks of previous methods: (a) It's non-parametric, like Kaiser-Squires and related weak lensing methods but unlike previous strong lensing work, (b) Error estimates are easy, (c) Lensing constraints remains linear in all regimes (strong, weak & intermediate), (d) No mass sheet degeneracy and no end (boundary) effects.

2 Outline of the method

The technique works with a pixellated mass distribution, i.e the mn -th pixel is a square tile^a with a surface mass density κ_{mn} in units of the critical density. For a source at an unlensed position β , the scaled time delay in a direction θ is

$$\tau(\theta) = \frac{1}{2}(\theta - \beta)^2 - \frac{D_{ls}}{D_s} \sum_{mn} \kappa_{mn} \psi_{mn}(\theta), \quad (1)$$

where $\psi_{mn}(\theta)$ (a known function) is how much the mn -th pixel would contribute to the potential.

^aOther types of pixels are also viable and produce similar mass maps.

Cluster lensing observations provide us with the following constraints:
 (i)– Image positions, say θ_1 , implying

$$\nabla\tau(\theta_1) = 0. \quad (2)$$

(ii)– Shear measurements at some θ_1 ; say the shear is observed to be at least k , and aligned along the $\theta_{x'}$ direction. This implies

$$k \left| \frac{\partial^2}{\partial\theta_{x'}^2} \tau(\theta_1) \right| \leq \left| \frac{\partial^2}{\partial\theta_{y'}^2} \tau(\theta_1) \right|. \quad (3)$$

Both types provide linear constraints on the unknowns β and κ_{mn} .

By quadratic programming, we can produce the mass maps that e.g., minimize M/L variation *while obeying the lensing constraints*. By minimizing M/L variations with respect to Monte-Carlo light distributions, we can estimate errors.

3 Abell 370

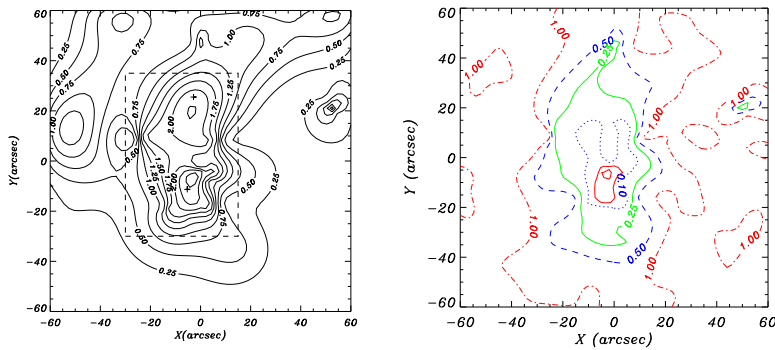


Figure 1: **Left:** Sky projected mass distribution of Abell 370. Mass enclosed by the dashed rectangle is $2.1 \times 10^{14} h_{50}^{-1} M_{\odot}$. **Right** Fractional uncertainty of the mass map.

Our reconstruction of Abell 370, using only the constraints from multiple images (strong lensing), is shown in Fig. 1. The reconstructed mass map predicted the bimodal nature of the cluster and robustly revealed features not associated with light (for more details see AbdelSalam et al 1997).

Our reconstruction indicates that the radial arc, recently discovered in the HST image, may be five images out of a seven image configuration.

4 Abell 2218

Our mass reconstruction for A2218, using the constraints from combined strong and weak lensing, is shown in Figure 2 (left) and the uncertainties are shown in Figure 3. Our reconstructions of the inner region of Abell 2218 uses both

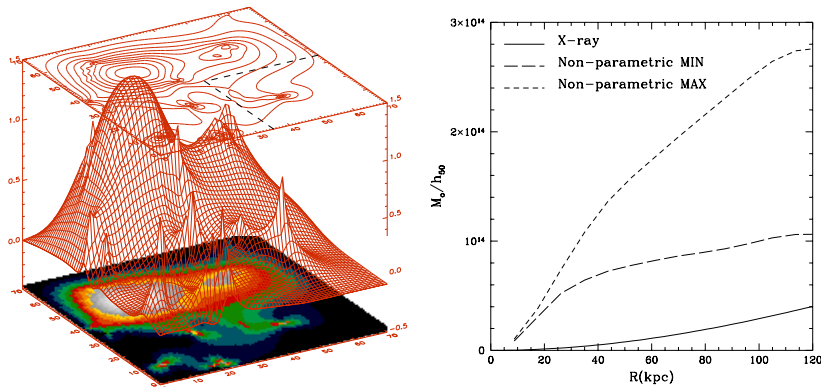


Figure 2: **Left:** Mass distribution of Abell 2218 in units of the critical surface density $3.1 \times 10^{10} h_{50}^{-1} M_{\odot} \text{arcsec}^{-2}$. The total mass in the region of the HST image is $2.74 \times 10^{14} h_{50}^{-1} M_{\odot}$. **Right:** The range of radial mass profiles for Abell 2218 allowed by lensing, and the mass radial profile from an X-ray model by Allen *et al*1997.

multiple image data (strong lensing) and singly imaged arc(lets) (weak lensing) from HST, plus spectroscopic redshifts from Ebbels *et al*1997. As far as we are aware this is the first mass reconstruction using strong and weak lensing simultaneously.

As Miralda-Escudé & Babul (1995) first noted, current X-ray mass models appear to underestimate the mass. Our results reinforce this conclusion: mass estimate from lensing is at least 2.5 times that from X-ray models (Figure 2 (right)). This may indicate the gas is partially supported by turbulence or magnetic fields, the gas is not uniform and isothermal or is not in equilibrium, but rather multiphase or has temperature gradient rising inwards; or the cluster is elongated along the line of sight.

Acknowledgements

HMA acknowledges the support of Overseas Research Scheme, Oxford Overseas Bursary and Wolfson College (Oxford) Bursary. LLRW acknowledges the sup-

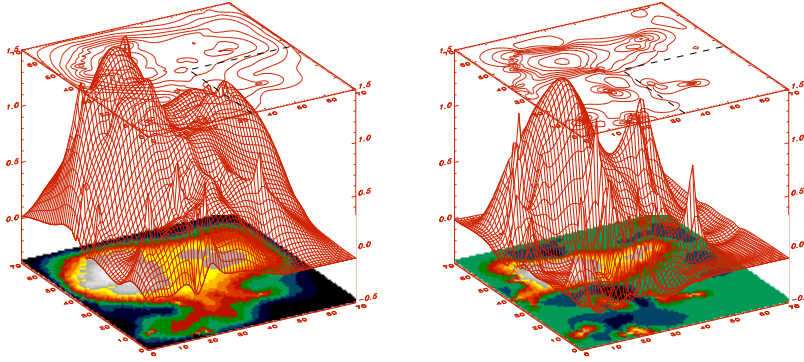


Figure 3: **Left:** Mass distribution of Abell 2218 plus (**left**) and minus (**right**) one standard deviation uncertainty.

port of PPARC fellowship at the IoA, Cambridge. HMA & LLRW thank the organisers of *Large Scale Structure: Tracks and Traces* for their kind hospitality.

References

1. AbdelSalam, H.M., Saha, P. & William, L.L.R., 1997, *MNRAS*, accepted; preprint astro-ph/9707207
2. Allen *et al*, 1997, private communications
3. Ebbels *et al*, 1997, preprint astro-ph/9703169
4. Kaiser, N. & Squires, G., 1993, *APJ*, 404, 441
5. Miralda-Escudé, J. & Babul, A., 1995, *APJ*, 449, 18